Inelastic scattering from Einstein modes of surface defects

C. W. Skorupka* and J. R. Manson
Department of Physics and Astronomy, Clemson University, Clemson, South Carolina 29634-1911
(Received 8 November 1989)

We consider the theory of inelastic scattering of atoms by isolated surface defects which have nearly dispersionless vibrational modes. Explicit calculations are carried out corresponding to the cases of chemisorbed CO on a Pt(111) surface, or heavy rare gases physisorbed on Pt(111) or Ag(111) surfaces. The multiphonon intensities are compared with available data. We show that the multiphonon intensities measured as a function of scattering angle exhibit broad oscillations similar to those observed in elastic scattering, and the polarization of the Einstein mode has a large effect on the envelope of these oscillations.

I. INTRODUCTION

Even the most carefully prepared surfaces always contain defects such as steps, kinks, and adsorbates. The defects may arise as a result of the surface preparation procedure or be deliberately created.[1] Understanding the nature of the surfaces requires an understanding of these defects. In scattering experiments, defects usually contribute to the diffusely reflected background and they cause a reduction in the intensity[2-4] or a broadening in the width[5-18] of the coherently scattered peaks. Recently, measurements of the elastic diffuse intensity of low-energy helium atoms at large momentum transfers have been demonstrated to give a large amount of information not only about the nature of individual defects,[19-21] but also about their distribution.[22,23] Measurements of the diffuse inelastic background in similar He scattering experiments have revealed the energies of special modes associated with isolated adsorbates or defects.[24,25]

We wish to consider here the inelastic scattering of low-energy atoms from surface defects; in particular, we consider defects which have isolated vibrational modes in the meV range. Such Einstein-like modes can arise in a number of different ways, for example, the low-energy vibrations of chemisorbed molecules such as CO on Pt.[24] Another example is the case of rare gases physisorbed on metal[26,27] or graphite[28] substrates. Additionally, clean but reconstructed surfaces can have features which vibrate with nearly Einstein behavior[25,29] and it has been proposed that such modes can be associated with the edges of steps.[30]

A defect on the surface breaks the two-dimensional symmetry, and for scattering events this means that it contributes to the diffuse intensity.[31] However, for Einstein vibrators the isolated frequency gives rise to a number of coherence effects which can arise when multiple quantum exchanges are appreciable.[32] In this paper we carry out explicit calculations of the inelastic scattering cross section for single and multiple quantum exchange of Einstein modes. The polarization of the vibrational displacement, whether it is parallel or perpendicular to the surface, leads to very significant differences in the pattern of scattered intensity. We find that multiple reflections between defect and substrate give rise to characteristic oscillations in the intensity as a function of scattering angle much in the same way as similar oscillations arise in the diffuse elastic scattering from isolated defects.[19,22] These oscillations can be used to obtain information on the size and shape of the defect profile.

II. THE INELASTIC TRANSITION RATE

In low-energy atom scattering all the incident atomic flux is backscattered, implying a strong interaction process which cannot be described by weak scattering theory such as the Born approximation. Furthermore, we are most interested in the amplitudes scattered with large parallel momentum transfers at large angles away from the specular direction. The appropriate starting point is the transition rate for a particle of initial momentum $\hbar\mathbf{k}_i$ going to a final state of momentum $\hbar\mathbf{k}_f$

$$w(\mathbf{k}_f,\mathbf{k}_i)=\frac{2\pi}{\hbar}\left\langle \sum_{n_f} |T_{fi}|^2 \delta(E_f-E_i)\right\rangle \tag{1}$$

where T_{fi} is the transition matrix, E_f and E_i are the final and initial energies of the total system of particle plus crystal, the sum is over final crystal states, and the average is over initial crystal states.[32] It will also be necessary to average (1) over the distribution of defects. The Van Hove transformation casts the transition rate into the form of a Fourier transform of a time-ordered correlation function

$$w(\mathbf{k}_f,\mathbf{k}_i)=\frac{1}{\hbar^2}\int_{\infty}^{-\infty} dt \exp[-i(\varepsilon_f-\varepsilon_i)t/\hbar] \times\langle T_{\rm if}(0)T_{fi}(t)\rangle , \tag{2}$$

in which the time dependence of the T operators is given in the interaction picture by the unperturbed crystal Hamiltonian, and ε_f and ε_i are the final and initial particle energies, respectively.

At this point we make three assumptions about the defects, they are all identical, they can be represented by nondeformable hard core scattering centers, and they are sufficiently dilute so that there is no appreciable multiple scattering between different defects. (However, multiple

scattering between defect and surface is important and must be accounted for.) At first glance the approximation of hard cores may seem overly restrictive, but it is justfied by the fact that we are interested in large angle scattering, in which the incoming atom strong samples the hard repulsive core. The soft van der Walls attractive part of the potential dominates the total cross section, but scatters only in a small range about the specular direction.[7-13] These assumptions allow us to write the transition matrix elements with respect to the particle states as

$$\langle \mathbf{k}_f | T(t) | \mathbf{k}_i \rangle = \tau(\mathbf{k}_f, \mathbf{k}_i) \sum_\alpha \exp[i\mathbf{k}\cdot\mathbf{R}_\alpha(t)] \tag{3}$$

where $\tau(\mathbf{k}_f,\mathbf{k}_i)$ is the transition matrix for scattering from an isolated defect and the summation runs over all defect sites. The wave-vector transfer $\mathbf{k}=\mathbf{k}_f-\mathbf{k}_i$ $=(\mathbf{K}_f-\mathbf{K}_i, k_{fz}+k_{iz})$ with capital letters referring to vectors parallel to the surface and small letters giving components in the z direction perpendicular to the surface. The position vector of the defect at site α which appears in the phase can be written as

$$\mathbf{R}_\alpha(t)=\mathbf{R}_\alpha+\mathbf{u}_\alpha(t) , \tag{4}$$

where $\mathbf{R}_\alpha$ is the time-independent equilibrium position and $\mathbf{u}_\alpha(t)$ is the displacement from equilibrium.

The defect vibration amplitude $\mathbf{u}_\alpha(t)$ is a linear combination of the modes of the substrate and the proper modes of the defect. To a good approximation we can write the amplitude as the sum of two terms

$$\mathbf{u}_\alpha(t)=\mathbf{u}^s_\alpha(t)+\mathbf{u}^d_\alpha(t) , \tag{5}$$

where $\mathbf{u}^d_\alpha(t)$ is the displacement due to the Einstein mode vibrations and $\mathbf{u}^s_\alpha(t)$ is the additional contribution due to the substrate vibrations. This implies that the defect simply rides on the substrate and that the two contributions are independent as expressed by

$$\langle \mathbf{k}\cdot\mathbf{u}^s_\alpha(t)\,\mathbf{k}\cdot\mathbf{u}^d_\alpha(0)\rangle = 0 . \tag{6}$$

The meaning of a dispersionless defect mode is that each defect vibrates at a single frequency and the vibrations between neighbors are uncorrelated. In addition, the single vibrational frequency will be associated with motion in a particular direction. These conditions are expressed as

$$\langle \mathbf{k}\cdot\mathbf{u}^d_\alpha(t)\,\mathbf{k}\cdot\mathbf{u}^d_\beta(0)\rangle = \langle \mathbf{k}\cdot\mathbf{u}^d(t)\,\mathbf{k}\cdot\mathbf{u}^d(0)\rangle\delta_{\alpha\beta}$$

$$= Q^2\langle u^d(t)u^d(0)\rangle\delta_{\alpha\beta} \tag{7}$$

where Q is the component of the wave vector $\mathbf{k}$ parallel to the direction of the one-dimensional vibrational displacement $u^d(t)$. In the case of physisorbed noble gases, the direction of the vibrational motion is normal to the surface.[26,27] For CO chemisorbed on a Pt(111) surface the Einstein frequency is identified with a wagging mode[20] and the displacement is parallel to the surface. However, even in this latter case we need consider only a single direction of momentum transfer since in most experiments the incident beam and detector are in the same plane with the normal to the surface.

If all displacements obey the harmonic approximation, the thermal averages in the transition rate of Eq. (2) can be readily carried out with the form of the transition operator (3). Together with the conditions (4)–(7) the result is

$$w(\mathbf{k}_f,\mathbf{k}_i)=\frac{1}{\hbar^2}\int_{-\infty}^{\infty} dt\,\exp[-i(\varepsilon_f-\varepsilon_i)t/\hbar]|\tau(\mathbf{k}_f,\mathbf{k}_i)|^2\exp[-2W^s(\mathbf{k})-2W^d(\mathbf{k})]$$
$$\times\left\langle\!\!\left\langle \sum_{\alpha;\beta}\exp[i\mathbf{k}\cdot(\mathbf{R}_\alpha-\mathbf{R}_\beta)]\exp[\langle \mathbf{k}\cdot\mathbf{u}^s_\alpha(0)\mathbf{k}\cdot\mathbf{u}^s_\beta(t)\rangle+\langle \mathbf{k}\cdot\mathbf{u}^d(0)\mathbf{k}\cdot\mathbf{u}^d(t)\rangle\delta_{\alpha\beta}]\right\rangle\!\!\right\rangle \tag{8}$$

where the double brackets signify an average over the distribution of defect positions. The two Debye-Waller factors arising from the substrate and defect motions, respectively, with exponents given by

$$2W^s(\mathbf{k})=\langle[\mathbf{k}\cdot\mathbf{u}^s_\alpha(t)]^2\rangle \text{ and } 2W^d(\mathbf{k})=\langle[\mathbf{k}\cdot\mathbf{u}^d_\alpha(t)]^2\rangle , \tag{9}$$

are independent of site index α if all defects are at the same position in the surface unit cell.

All inelastic exchanges will arise from the displacement correlation functions appearing in the final exponentials of Eq. (8). Since we are considering here the inelastic contributions due to the Einstein modes, we will ignore all contributions from the substrate modes except for their contribution to the Debye-Waller factor. For an Einstein mode the frequency distribution function is a δ function in the Einstein frequency Ω, and the displacement correlation function is

$$\langle u^d(0)u^d(t)\rangle=\frac{\hbar}{2M\Omega}\{n(\Omega)e^{i\Omega t}+[n(\Omega)+1]e^{-i\Omega t}\} \tag{10}$$

where M is the defect mass and $n(\Omega)$ is the Bose-Einstein function. In the multiphonon inelastic interactions with an Einstein oscillator, all processes involving equal numbers of creation and annihilation events contribute to the inelastic signal. All such events can be summed in the transition rate of Eq. (9), and for a random distribution of site positions the result is

$$w^0(\mathbf{k}_f,\mathbf{k}_i)=\frac{2\pi}{\hbar}\eta|\tau(\mathbf{k}_f,\mathbf{k}_i)|^2\exp[-2W^s(\mathbf{k})-2W^d(Q)]$$
$$\times I_0\left[\frac{Q^2\hbar}{M\Omega}\sqrt{n(\Omega)[n(\Omega)+1]}\right]\delta(\varepsilon_f-\varepsilon_i) \tag{11}$$

where η is the defect density and $I_\alpha(x)$ is the modified Bessel function of order α. Equation (11) has been used to explain the large angle diffuse elastic scattering of helium atoms from steps and adsorbates.[20,22] Additional fine structure details in the observed elastic intensity from steps have been discussed in terms of lattice gas interfer-

ence arising from nonrandom distributions of positions.[22,23]

Inelastic contributions to the transition rate (8) involving exchange of α phonons also have contributions coming from all higher-order processes. Because of the vibrational incoherence of the Einstein oscillators as expressed in Eq. (7) there are no coherences arising from correlations in position distributions, and the averaged summation over defect sites in (8) yields a factor of η. All order of phonon exchanges can then be summed to give an expression for the inelastic transition rate for the exchange of α phonons:[21]

$$w^{\alpha}(\mathbf{k}_f,\mathbf{k}_i)=\frac{2\pi}{\hbar}\eta|\tau(\mathbf{k}_f,\mathbf{k}_i)|^2\exp[-2W^s(\mathbf{k})-2W^d(\mathbf{Q})]I_{\alpha}\left[\frac{Q^2\hbar}{M\Omega}\sqrt{n(\Omega)[n(\Omega)+1]}\right]$$
$$\times(\delta(\varepsilon_f-\varepsilon_i-\alpha\hbar\Omega)\{n(\Omega)/[n(\Omega)+1]\}^{\alpha/2}+\delta(\varepsilon_f-\varepsilon_i+\alpha\hbar\Omega)\{[n(\Omega)+1]/n(\Omega)\}^{\alpha/2}) . \quad (12)$$

Equation (12) can be viewed as consisting of three parts, the δ functions for creation and annihilation which give the conservation of energy between particle and crystal, a form factor for the scattering center $2\pi|\tau(\mathbf{k}_f,\mathbf{k}_i)|^2\hbar$, and the remaining factors which constitute an inelastic structure factor. At low temperatures only creation processes are possible and the inelastic structure factor reduces to the Poisson distribution $\exp[-2W^s(\mathbf{Q})]e^{-x}x^{\alpha}/\alpha!$, with $x=Q^2\hbar/2M\Omega$, modified by the Debye-Waller factor for the substrate motion. At high temperatures the Einstein mode Debye-Waller factor is partially canceled by the Bessel function and the temperature dependence goes as $\exp[-2W^s(\mathbf{Q})]/\sqrt{T}$.

The diffuse inelastic intensity arising solely from the defect Einstein modes is contained in Eq. (12). In order to make comparisons with experiment, the form factor of the specific defect must be evaluated, and we consider that question in the next section.

III. THE FORM FACTOR

The form factor in the transition rate of Eq. (12) above is essentially the square modulus of the transition matrix for scattering by a single defect. In general, the wave function in the asymptotic region far from the surface is of the form

$$\Psi_i(\mathbf{R},z\to\infty)=\exp(-ik_{iz}z+i\mathbf{K}\cdot\mathbf{R})|i\rangle + \sum_{\mathbf{K};n} C_n(\mathbf{K})\exp[i(\mathbf{K}_i+\mathbf{K})\cdot\mathbf{R}+ik_{fz}z]|n\rangle \quad (13)$$

with $k_{fz}=[k_{iz}^2+\mathbf{K}_i^2-(\mathbf{K}_i-\mathbf{K})^2+2m\Omega_n/\hbar]^{1/2}$ where $\hbar\Omega_n$ is the total energy difference between the initial crystal state $|i\rangle$ and the final crystal state $|n\rangle$. The coefficients of the outgoing scattered waves of (13) are proportional to the transition matrix

$$C_n(\mathbf{K})=\frac{m}{L^2\hbar^2|k_{fz}|}\tau(\mathbf{k}_f,\mathbf{k}_i)e^{i\phi} \quad (14)$$

where ϕ is an unimportant phase and L^2 is the area of the surface.

Since, as discussed above, the large angle diffuse scattering is predominantly caused by the repulsive hard core of the potential, we will model the form factor by an infinitely hard repulsion calculated in the eikonal approximation.[33] In this case the amplitude $C_n(\mathbf{K})$ is determined by applying the boundary condition that the wave function vanish at the profile of the hard surface located at the position $z=\xi(\mathbf{R})$:

$$\Psi_i(\mathbf{R},z=\xi(\mathbf{R}))=0 . \quad (15)$$

Usually there are multiple semiclassical hits which may contribute to scattering at a given final angle, but the eikonal approximation only accounts for single hits. An important example occurring in defect scattering is a second hit involving a backreflection by the mirror surface. Such terms are explicitly accounted for by adding an "image" contribution to the scattering amplitude corresponding to the transfer of perpendicular momentum $q'=k_{iz}-k_{fz}$ as opposed to $q=k_{iz}+k_{fz}$ for the directly scattered part. The evaluation of $C_n(\mathbf{K})$ after applying the boundary condition (15) directly to the form of the wave function (13) is straightforward, and the final result is

$$C_n(\mathbf{K})=-\frac{1}{L^2}\int d\mathbf{R}\,e^{-i\mathbf{K}\cdot\mathbf{R}}(e^{-iq\xi(\mathbf{R})}-e^{-iq'\xi(\mathbf{R})}-1) . \quad (16)$$

The integral in (16) runs only over the region of the isolated defect; in the language of semiclassical scattering the first two terms in the integrand are the direct and backreflected illuminated face contributions, respectively, and the final term is the shadow or Fraunhofer part. There is also a term in $C_n(\mathbf{K})$ involving an integral over the entire infinite flat surface, but since that only contributes to the amplitude near the specular direction it is of no interest here.

The simplest choice for the defect profile function is a hemisphere of radius a resting on top of the surface, in which case

$$\xi(\mathbf{R})=\begin{cases}0, & R\geq a\\ (a^2-R^2)^{1/2}, & R<a .\end{cases} \quad (17)$$

With this choice of profile the Fraunhofer term of the amplitude (16) can be evaluated exactly. The two illuminated face terms admit to an analytic expression in the stationary phase approximation. Using the notation

$$\mathbf{k}\cdot\hat{\mathbf{n}}=[k_f^2+k_i^2+2k_fk_i\cos(\theta_f+\theta_i)]^{1/2} ,$$
$$\mathbf{k}'\cdot\hat{\mathbf{n}}'=[k_f^2+k_i^2-2k_fk_i\cos(\theta_f-\theta_i)]^{1/2} \quad (18)$$

the result is

$$C_n(\mathbf{K})=\frac{2\pi}{L^2}\left[\frac{ie^{-ia\mathbf{k}\cdot\hat{\mathbf{n}}}}{a\mathbf{k}\cdot\hat{\mathbf{n}}}-\frac{ie^{-ia\mathbf{k}'\cdot\hat{\mathbf{n}}'}}{a\mathbf{k}'\cdot\hat{\mathbf{n}}'}+\frac{J_1(Ka)}{K}\right]. \quad (19)$$

Equation (19) provides a useful closed form approximation for the scattering amplitude. In actual practice we found it more convenient to obtain the amplitude by direct numerical integration of Eq. (16), a procedure which is valid for smaller values of ka than the stationary phase approximation of Eq. (19).

IV. CALCULATIONS AND COMPARISON WITH EXPERIMENT

For making comparisons with experiment we first note that the quantity which would normally be measured is the differential reflection coefficient which is obtained upon multiplying the transition rate $w(\mathbf{k}_f,\mathbf{k}_i)$ by the density $\rho=m|\mathbf{k}_f|/8\hbar^2\pi^3$ of final states in phase space and dividing by the incident flux $j_i=\hbar k_{iz}/m$. In addition other factors may be necessary depending on peculiarities of the experimental configuration. For example, if the detector acceptance angle subtends only a small portion of a surface fully illuminated by the incident beam, there will be an additional factor of $1/\cos\theta_f$ to account for the increase of surface area viewed as the polar angle θ_f of the detector is varied.[19]

We must also evaluate the Debye-Waller factors. The Debye-Waller exponent for the defect mode (9) is readily evaluated from the displacement correlation function (10)

$$W^d(Q)=\frac{\hbar Q^2}{2M\Omega}[n(\Omega)+\tfrac{1}{2}]. \quad (20)$$

For the contribution to the Debye-Waller factor from the substrate, it has been shown that only the vibrations normal to the surface play an important role. Furthermore, the effect of the attractive well of depth D in the potential should be taken into account. We parametrize the Debye-Waller exponent as

$$W^s(\mathbf{k})=\lambda\hbar\Omega[(k_{iz}+k_{fz})^2+\gamma][n(\Omega)+\tfrac{1}{2}]/k_B \quad (21)$$

where k_B is the Boltzmann constant. In Eq. (21) the parameter γ contains the well depth correction and is slightly different from the usual practice of refracting the incident and scattered semiclassical beams through a relation of the form $k_{fz}\rightarrow k_{fz}^*=(k_{fz}^2+2mD/\hbar^2)^{1/2}$ and similarly for k_{iz}.[34] In the comparisons below the parameters λ and γ are chosen by matching (21) to the available experimental data for thermal attenuation of the elastic specular beams.[34]

Figure 1 shows a calculation of the differential reflection coefficient for the scattering of helium by adsorbates on a hard surface using the form factor calculated from the hemispherical defect profile of Eq. (17) with $a=2.4$ Å. All incident conditions and parameters are chosen to match the experimental conditions for CO adsorbed on a Pt(111) surface,[20,24] and are given in Table I. Both the diffuse elastic and the single phonon creation inelastic intensities are shown. The Einstein energy $\hbar\Omega$ is 6 meV and corresponds to the lowest-energy vibrational mode of adsorbed CO on Pt, all other modes being too high in energy to be detected in the experiment.[24] This lowest-energy mode is a "wagging" mode in which the motion is parallel to the surface and this means that the momentum Q is the parallel momentum transform K in the scattering direction.

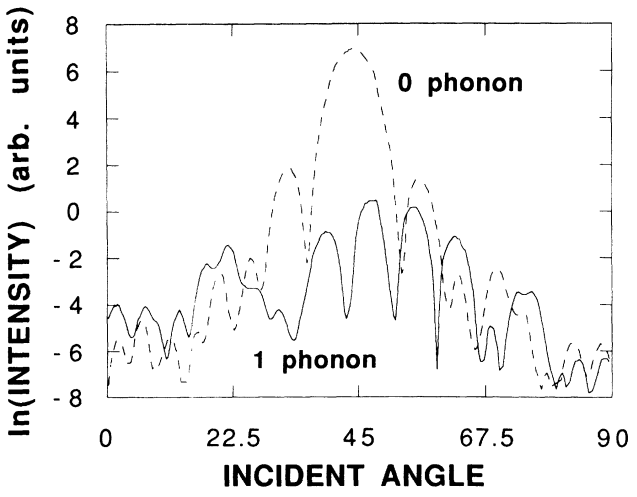

FIG. 1. The differential reflection coefficient as a function of incident angle for the elastic and one phonon annihilation peak intensities for He with $E_i=18.3$ meV scattering from a model of CO adsorbed on a smooth Pt surface. The detector angle is fixed at $\theta_{SD}=90°$ with respect to the incident angle in the sagittal plane.

The most immediate observation from Fig. 1 is that the single phonon inelastic intensity exhibits reflection symmetry oscillations in much the same way as does the elastic intensity. These arise from the quantum-mechanical interference between the first two (illuminated face) terms in the scattering amplitude of Eq. (19). The single phonon intensity is usually smaller than the elastic intensity, but this is not always the case as a crest of the inelastic intensity may fall on a trough of the elastic signal. Similarly, we find that the two phonon signal or even the three phonon signal can have a stronger intensity than the elastic or single phonon intensity at certain angles. This implies that when attempting to measure a particular multiphonon signal it is of interest to choose an angle at which its form factor is large.

Just as is the case for the elastic signal, the positions and relative amplitudes of the inelastic reflection symmetry oscillations give information on the size, profile shape, and rainbow positions of the defect hard core. We have noted that the relative positions of the oscillations in the various multiphonon intensities are sensitive to parameter changes, in this case changes in hemisphere radius and incoming momentum.

Figures 2 and 3 illustrate the difference in nature between the diffuse inelastic scattering of helium from a defect which vibrates parallel to the surface and one which vibrates perpendicularly. Figure 2 is for the CO/Pt pa-

TABLE I. The calculated inelastic structure factor compared with available experimental intensity measurements for several systems. Intensities are normalized to the elastic intensity for the case of CO/Pt, and normalized to the single phonon creation intensity for all other cases. T_S is the surface temperature and the parameters of the Debye-Waller factor of Eq. (21) are $\lambda = 1.27 \times 10^{-5}$ Å^2 K^{-1} and $\gamma = 46$ Å^{-2} (corresponding to a well depth of approximately 6 meV).

ΔE (meV)	α	I/I_0 (expt)	I/I_0 (calc)	E_i (meV)	θ_i (deg)	θ_{SD} (deg)	T_s (K)
			CO/Pt(111)[24]				
12	2	0.016	0.026	18.3	29.9	90	300
6	1	0.067	0.15				
0	0	1	1				
−6	−1	0.16	0.14				
−12	−2	0.08	0.0035				
			Kr/Pt(111)[26]				
3.7	1	0.13	0.23	18.3	45	83	25
−3.7	−1	1	1				
−7.3	−2	0.28	0.36				
			Kr/Ar(111)[27]				
2.9	1	0.4	0.27	18.0	45	83	24
−2.9	−1	1	1				
−5.8	−2	0.25	0.6				
−8.7	−3	0.05	0.2				
			Xe/Ag(111)[27]				
2.8	1	0.3	0.27	18.0	60	73	24
−2.8	−1	1	1				
−5.4	−2	0.3	0.4				
−8.3	−3	0.1	0.14				
			Ar/Ag(111)[27]				
3.67	1	0.25	0.18	18.0	45	83	22.5
−3.67	−1	1	1				
−7.18	−2	0.25	0.6				
−10.6	−3	0.05	0.4				

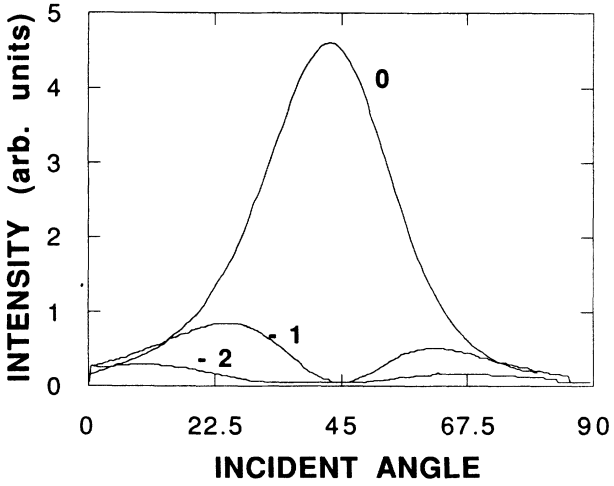

FIG. 2. The inelastic structure factor as a function of incident angle for the elastic, and one and two phonon creation peak intensities. All parameters are the same as for the case of He scattered by CO adsorbed on Pt shown in Fig. 1.

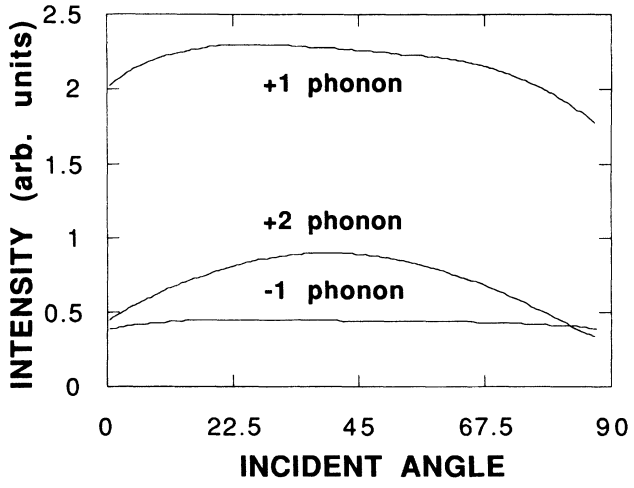

FIG. 3. The inelastic structure factor as a function of incident angle for the one phonon creation, and the one and two phonon annihilation peak intensities for the case of He scattered by Kr adsorbed on a Pt(111) substrate. The incident energy is 18.3 meV, the surface temperature is 25 K, and the fixed angle between incident beam and detector is $\theta_{SD} = 83°$.

rameters of Fig. 1, and plotted is the transition rate with the form factor factored out. What is left is essentially the inelastic structure factor which is shown for the zero, one, and two phonon creation processes. The decrease in intensity for larger numbers of phonon exchange is mainly due to the Debye-Waller factor. The inelastic intensity for the exchange of α phonons vanishes near the specular angle at the point where Q, the parallel momentum exchange, is zero. The factor of Q^2 in the Bessel function of Eq. (12) shows that the small Q dependence goes as $Q^{2\alpha}$. Table I gives a comparison between the calculations as shown in Fig. 2 and experiment[24] at the measured angles, with all intensities normalized to the elastic intensity. The qualitative trend of the calculations agrees with that of the experiment, and the actual relative intensities are in good agreement considering that the effects of the form factor are ignored. Figure 3 is similar to Fig. 2 except that it is for the case of Kr adsorbed on a Pt(111) substrate.[26] In this case the vibration is normal to the surface and Q is the normal momentum transfer which is always greater than zero under any experimentally achievable incidence conditions. Thus the signature of this case is quite different from the parallel vibration case above. The elastic intensity is not shown because most of the experiments reported for rare gases on metal substrates are with high coverages of the adsorbates[26,26,35] and our elastic theory is not valid for this case. However, for inelastic scattering our theory remains valid for a combination of two reasons, (i) the normally vibrating Einstein modes of adjacent adsorbates are decoupled and hence still exhibit the incoherence expressed in Eq. (7) (this is not the case for the modes of this system associated with parallel polarization, but these modes are not seen by helium scattering), and (ii) there is experimental evidence that multiple scattering between neighboring adsorbates does not occur in the inelastic exchanges.[36] This experimental evidence consists of He reflected from well-mixed solutions with near monolayer coverage of Kr and Xe on a Pt(111) substrate. The inelastic intensity consisted of multiples of the Kr frequency and multiples of the Xe frequency, but no mixtures of the two, indicating that there was no multiple scattering between neighboring defects. Table I also gives the comparison of the calculations of Fig. 3 with experiment and similarly for a number of other available data. All comparisons except for that with CO are normalized to the single phonon creation intensity for the reasons stated above. The experimental intensities are obtained by comparing relative peak heights to background levels as obtained from Refs. 24, 26, and 27. In all cases the qualitative trend of the calculations is correct in spite of the fact that the form factor has been ignored.

V. CONCLUSIONS

We have considered the diffuse, multiphonon inelastic scattering intensities for very-low-energy atoms incident on a dilute distribution of defects on a flat surface. When these defects have dispersionless, or Einstein vibrational modes, the energy-resolved differential reflection coefficient has peaks corresponding to each multiphonon exchange. When a given multiphonon peak is measured as a function of scattering angle or momentum exchange, it exhibits a series of broad oscillations whose origin is the same as the reflection symmetry oscillations observed in the diffuse elastic intensity.[20] The oscillations are the result of interference between two or more semiclassical paths, arising either from a combination of direct scattering from the defect and double scattering from the defect and surface, or from a supernumerary rainbow situation in which there are more than one possible paths of scattering from the defect hard core profile. The position and relative intensity of these oscillations depend strongly on the size and shape of the hard core profile of the defect.

A single frequency Einstein mode will have a polarization direction, usually either parallel or perpendicular to the surface. Parallel and perpendicularly polarized modes exhibit quite different signatures. The intensity for the exchange of α phonons scattered from a parallel mode is proportional to $K^{2\alpha}$ where K is the parallel momentum exchanged, hence the intensity vanishes strongly near the specular direction where K is small. For perpendicular modes the relevant momentum exchange is in the perpendicular direction and this does not vanish under normal experimental conditions, so the intensity tends to be largest for angles in the neighborhood of the specular direction.

We have carried out calculations in which the defect is an adsorbate with a hard core profile modeled by a hemisphere on a flat surface. These clearly indicate the reflection symmetry oscillations and the polarization effects. Direct comparison with experiment is made for a number of different systems and although the number of angles measured for each system is very limited, the agreement is encouraging. Our calculations indicate that more detailed experiments will give information not only on the energies and polarizations of the multiphonon or overtone frequencies, but also will have the capability of giving detailed information on the nature of the defect.

ACKNOWLEDGMENTS

We would like to thank J. P. Toennies, B. J. Hinch, A. M. Lahee, and Ch. Wöll for helpful discussions.

*Present address: Naval Research Laboratory (Code 6341), Washington, D.C. 20385-5000.

[1]B. Poelsema and G. Comsa, in *Springer Series in Surface Science* (Springer-Verlag, Berlin, in press).

[2]M. Henzler, in *Electron Spectroscopy for Surface Analysis*, edited by H. Ibach (Springer, Berlin, 1977).

[3]J. Lapujoulade, Surf. Sci. **108**, 526 (1981).

[4]L. K. Verheij, B. Poelsema, and G. Comsa, Surf. Sci. **162**, 858 (1985).

[5]D. L. Smith and R. P. Merrill, J. Chem. Phys. **52**, 5861 (1970).

[6]B. F. Mason, R. Caudano, and B. R. Williams, Phys. Rev. Lett. **47**, 1141 (1981); J. Chem. Phys. **77**, 562 (1982).
[7]B. Poelsema, G. Mechtersheimer, and G. Comsa, Surf. Sci. **111**, 519 (1981).
[8]B. Poelsema, R. L. Palmer, G. Mechtersheimer, and G. Comsa, Surf. Sci. **117**, 60 (1982).
[9]B. Poelsema, R. L. Palmer, and G. Comsa, Surf. Sci. **123**, 152 (1982).
[10]B. Poelsema, S. T. de Zwart, and G. Comsa, Phys. Rev. Lett. **49**, 578 (1982); **51**, 522 (1983).
[11]B. Poelsema, R. L. Palmer, S. T. de Zwart, and G. Comsa, Surf. Sci. **126**, 641 (1983).
[12]B. Poelsema, L. K. Verheij, and G. Comsa, Phys. Rev. Lett. **49**, 1731 (1982).
[13]B. Poelsema, L.K. Verheij, and G. Comsa, Phys. Rev. Lett. **51**, 2410 (1983).
[14]J. Ibanez, N. Garcia, J. M. Rojo, and N. Cabrera, Surf. Sci. **117**, 23 (1982).
[15]J. Ibanez, N. Garcia, and J. M. Rojo, Phys. Rev. B **28**, 3164 (1982).
[16]T. Engel, J. Chem. Phys. **69**, 373 (1978).
[17]D. H. Winicur, J. Hurst, C. A. Becker, and L. Wharton, Surf. Sci. **109**, 263 (1983).
[18]H. Wilsch and K. H. Rieder, J. Chem. Phys. **78**, 7491 (1983).
[19]A. M. Lahee, J. R. Manson, J. P. Toennies, and Ch. Wöll, Phys. Rev. Lett. **57**, 471 (1986).
[20]A. M. Lahee, J. R. Manson, J. P. Toennies, and Ch. Wöll, J. Chem. Phys. **88**, 7194 (1987).
[21]B. J. Hinch, C. Koziol, J. P. Toennies, and G. Zhang (unpublished).
[22]C. W. Skorupka and J. R. Manson, Phys. Rev. B **41**, 8156 (1990).
[23]B. J. Hinch and J. P. Toennies (unpublished).
[24]A. M. Lahee, J. P. Toennies, and Ch. Wöll, Surf. Sci. **177**, 371 (1986).
[25]U. Harten, J. P. Toennies, and Ch. Wöll, Phys. Rev. Lett. **57**, 2497 (1986).
[26]K. Kern, P. Zeppenfeld, R. David, and G. Comsa, Phys. Rev. B **35**, 886 (1987).
[27]K. D. Gibson and S. Sibener, J. Chem. Phys. **88**, 7862 (1988).
[28]T. H. Ellis, G. Scoles, U. Valbusa, H. Jonsson, and J. H. Weare, Surf. Sci. **155**, 499 (1985).
[29]O. L. Allerhand and E. J. Mele, Phys. Rev. Lett. **59**, 657 (1987).
[30]A. A. Maradudin, E. W. Montroll, and G.H. Weiss, *Theory of Lattice Dynamics in the Harmonic Approximation* (Academic, New York, 1963), Suppl. 4.
[31]J. R. Manson and V. Celli, Phys. Rev. B **39**, 3605 (1989).
[32]J. R. Manson, Phys. Rev. B **37**, 6750 (1988).
[33]U. Garibaldi, A. C. Levi, R. Spadacini, and G. W. Tommei, Surf. Sci. **48**, 649 (1975).
[34]V. Bortolani, V. Celli, A. Franchini, J. Idiodi, and G. Santoro, Phys. Rev. B **35**, 6029 (1987).
[35]K. D. Gibson and S. Sibener, J. Chem. Phys. **83**, 4256 (1985).
[36]K. Kern, P. Zeppenfeld, R. David, and G. Comsa, Phys. Rev. B **35**, 886 (1987).